

The Flowing-Afterglow Technique, an Approach to the Study of Polymer Thermal Degradation

MICHAEL L. MATUSZAK and GENE W. TAYLOR, *University of California, Los Alamos National Laboratory, Los Alamos, New Mexico 87545*

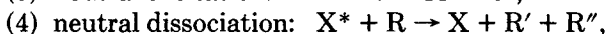
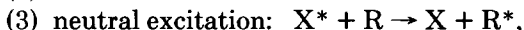
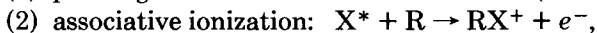
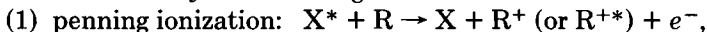
Synopsis

We describe here a relatively new analytical method¹⁻³ for following the thermal reaction history of polymers by quantitatively detecting the evolution of gases and some volatiles by flowing-afterglow spectroscopy. The thermal and oxidative stability of common plastics in many industrial and defense applications is of wide interest. We have studied the evolution of moisture and carbon dioxide from Li₂CO₃/Orlon-filled diallyl phthalate (DAP) composites and have briefly examined the thermal stability of Estane 5703, a polyester-based thermoplastic polyurethane. The results of these preliminary studies have shown the utility of FLAG spectroscopy as a means toward our understanding polymer stability and lifetimes in specified environments. FLAG data, combined with differential scanning calorimetry (DSC) and thermogravimetric analysis (TGA) data, have extended our knowledge of Li₂CO₃/Orlon/DAP and Estane aging processes. The DAP composites evolve H₂O and CO₂ at near ambient temperatures, and we have described the kinetics of gas evolution and have attempted to describe the mechanism of thermal degradation. In the 25–120°C temperature range Estane 5703 evolves CO₂ as a decomposition product and some adsorbed moisture.

INTRODUCTION

Industrial and military plastics are required to survive their functional environments for their specified service lifetime. The mechanisms and kinetics of the degradation of plastics under service conditions (that is, 25–35°C in air) are difficult to determine. Very sensitive analytical methods are required.

The flowing-afterglow technique is potentially able to add greatly to the understanding of ambient temperature degradation processes of commonly used plastics and composites. The sensitivity of this technique and its dynamic nature make it attractive as a means for studying the thermal aging processes and kinetics of polymers. This method utilizes the energy-transfer reactions of rare-gas, metastable atoms from a fast-flowing, rare-gas plasma with the reagents of interest. The method described here is not useful for reagent concentrations beyond ~1000 ppm, but does extend below the 1 ppm level depending upon the level of sophistication of the photon detection method. The reactions of utility are summarized by the following:



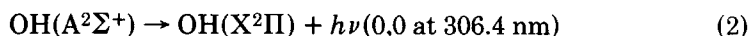
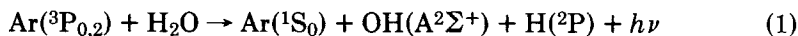
where * denotes electronic excitation and R' and R'' are molecular fragments of R, the evolved volatile of interest. Reactions 1, 3, and 5 are of particular in-

terest, because they yield sensible emissions from reagents of their fragments that can be spectroscopically detected with high sensitivity.

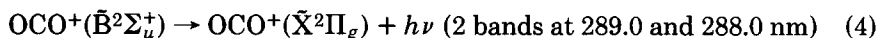
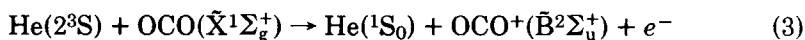
The flowing-afterglow technique was pioneered by Robertson et al.²⁻⁴ for He(2^3S) and Ar($3P_{0,2}$) and by Schmeltkopf and Broida⁵ for He(2^3S). Many of the important techniques of analysis were found in a review by Stedman and Setser.^{6,7} We applied the afterglow method to the analysis and detection of volatile products from the pyrolysis of a diallyl-phthalate composite and a thermoplastic polyurethane. The objective was to identify the decomposition products of both materials and to study their kinetics and mechanisms.

The specific reactions for the decomposition products of interest are as follows:

H₂O:



CO₂:



The primary reaction (3) is a Penning ionization reaction with the excited ($\tilde{B}^2\Sigma_u^+$) state formed directly in the reaction. Two prominent peaks in the 290-nm regions result from the $\tilde{B}^2\Sigma_u^+ \rightarrow \tilde{X}^2\Pi_g$ decay process. Note that the argon metastable was used for H₂O detection and the helium metastable was used for CO₂ detection. The helium metastable will excite both CO₂ and H₂O,

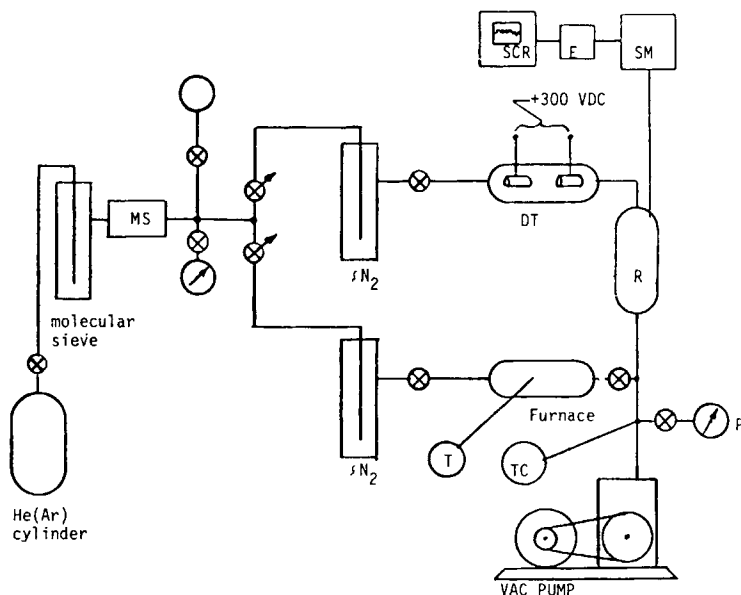


Fig. 1. Flowing-afterglow experiment setup: MS = molecular sieve trap; DT = discharge tube; SM = scanning monochromator; E = electron meter; SCR = strip chart recorder; R = reactor; T = temperature sensing thermocouple; P = pressure gauges; TC = pressure sensing thermocouple.

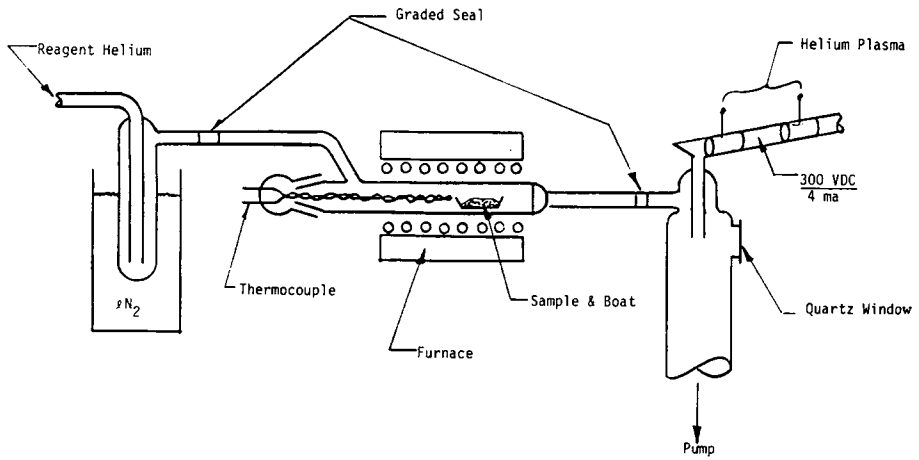


Fig. 2. Sample chamber.

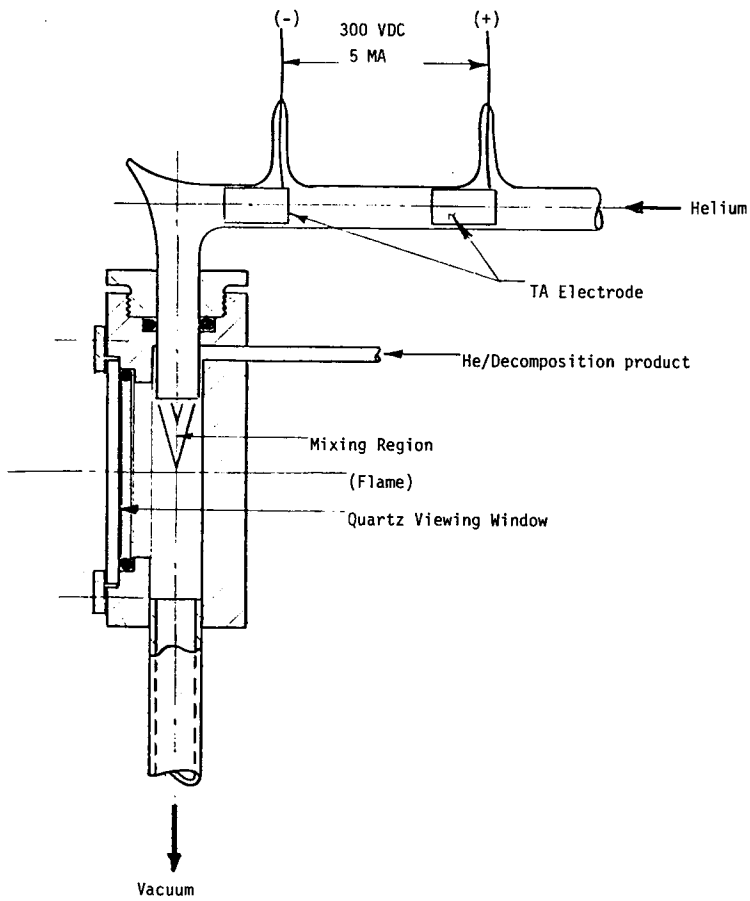


Fig. 3. Mixing chamber.

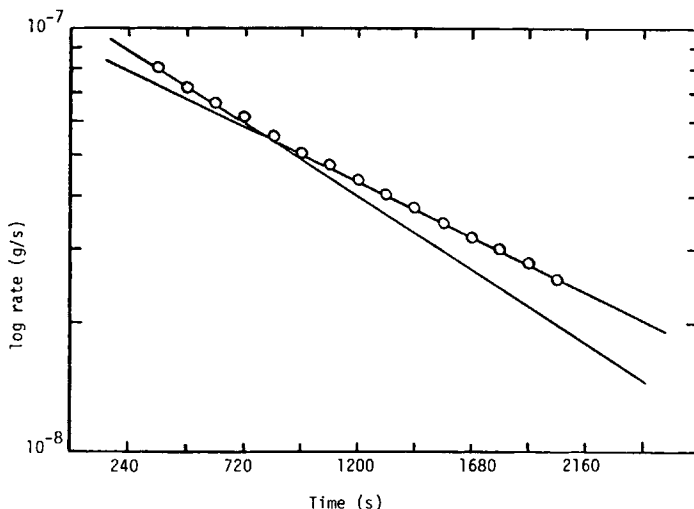


Fig. 4. Moisture release from DAP. (O) experimental curve, 60°C.

and the emission bands overlap somewhat. The argon metastable will only excite the H_2O .

EXPERIMENTAL

Materials

The first material used in this study was a diallyl phthalate composite containing 17 wt % Li_2CO_3 , 24.9 wt % Orlon fiber, and 0.01 wt % tertiarybutyl perbenzoate catalyst. The test specimens were 2.54-cm \times 0.64-cm \times 0.32-cm rectangles that were machined from a larger piece that was reaction-molded at 140°C and 16.5 MPa for 30 min.

Estane 5703, a polyester-based thermoplastic polyurethane elastomer supplied by B. F. Goodrich, was the second material tested. Estane 5703 is formed from reaction of a poly(tetramethylene adipate) glycol, 1,4-butanediol, and 4,4'-diphenylmethane diisocyanate (MDI).

Method

The apparatus used in this study is illustrated schematically in Figure 1. Reagent-grade helium was purified by passage through multiple-baffle molecular-sieve (Linde 5A) traps at -195°C and through low-pressure glass traps at -195°C . The purified helium flowed through a cold-cathode discharge maintained by hollow tantalum electrodes at 300 Vdc and 3–4 mA. A high capacity, two-state mechanical pump permitted helium flows of $\sim 1 \times 10^3 \mu\text{mol/s}$ at ~ 400 Pa discharge tube pressure. Spectra were taken with an MPI 0.45-m scanning monochromator equipped with a 1P28 phototube and SSR/PAR photon counter. Detailed sketches of the furnace and reaction chamber are shown in Figures 2 and 3.

The argon metastable was similarly produced, except the high-pressure, mo-

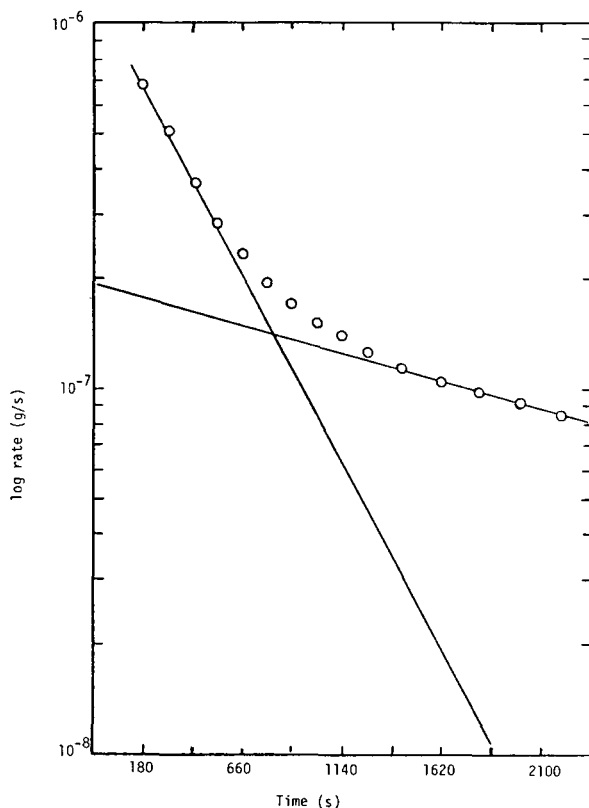


Fig. 5. Moisture release from DAP. (O) experimental curve, 100°C.

TABLE I
DAP Moisture Release Rate Constants

$T(^{\circ}\text{C})$	k_1^a (average) ^b	k_2^a (average) ^b	k_1/k_2
60 ± 1	$2.12 \pm 0.23 \times 10^{-3}$	$3.34 \pm 0.70 \times 10^{-4}$	6.35
70 ± 1	$2.22 \pm 0.58 \times 10^{-3}$	$4.83 \pm 1.1 \times 10^{-4}$	4.60
80 ± 1	$1.61 \pm 0.04 \times 10^{-3}$	$4.34 \pm 0.49 \times 10^{-4}$	3.71
90 ± 1	$1.43 \pm 0.27 \times 10^{-3}$	$5.99 \pm 0.94 \times 10^{-4}$	2.39
100 ± 1	$1.27 \pm 0.22 \times 10^{-3}$	$4.36 \pm 0.36 \times 10^{-4}$	2.91

^a k is the rate constant in s^{-1} .

^b The reported values are the average of 2-3 values and are reported with their average deviation.

lecular-sieve-packed traps were held at -78°C . Argon flows were also $\sim 1 \times 10^3$ $\mu\text{mol/s}$ at a flow-tube pressure of 650 Pa.

Calibration

The flowing-afterglow experimental apparatus was calibrated for water and carbon dioxide by the method of Taylor and Andrews.⁸

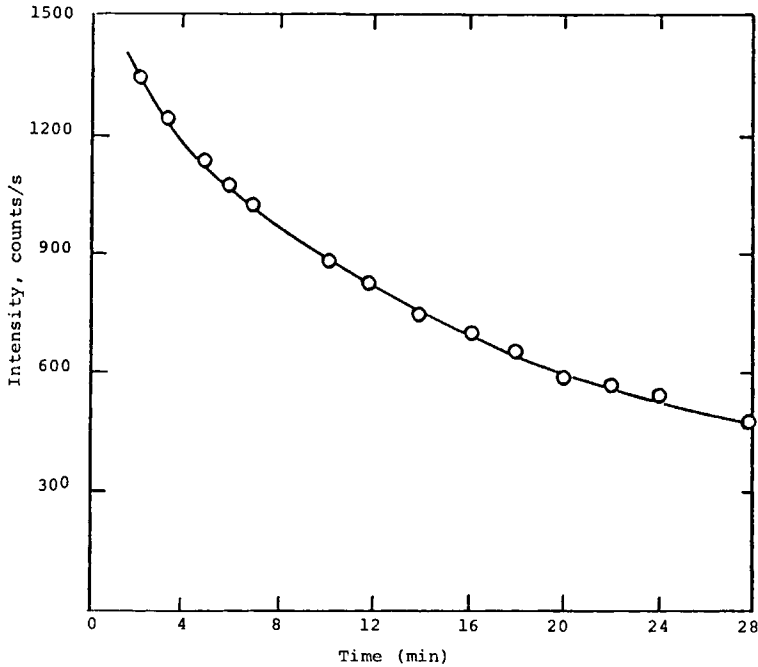


Fig. 6. Drying curves of DAP at 75°C using flowing-afterglow analysis. (O) Li_2CO_3 filter.

RESULTS AND DISCUSSION

Diallyl Phthalate Composite

The objective of the study on the DAP composite was to use the flowing-afterglow technique to study the kinetics and mechanism of moisture release. The test specimens were vacuum dried at 110°C for 24 h and were exposed to 10% relative humidity for times varying from 1 day to 21 days.

The moisture loss is the time exponential related to the rate constant by the following:

$$(\text{H}_2\text{O})_t = (\text{H}_2\text{O})_0 e^{-kt} \quad (5)$$

where $(\text{H}_2\text{O})_t$ is the moisture in the DAP composite at any time t (s), $(\text{H}_2\text{O})_0$ is the initial moisture content, and k (s^{-1}) is the first-order rate constant. Figures 4 and 5 show $\log d[(\text{H}_2\text{O})_t/dt]$ (g/s) vs. time (s) at 60°C and 100°C, respectively. Two exponential equations are necessary to fit the total experimental curve, suggesting that the DAP composite loses water by two different processes. At 60°C the observed rate equation is

$$\text{rate } 60^\circ\text{C} = 1.07 \times 10^{-7} e^{-2.12 \times 10^{-3}t} + 9.29 \times 10^{-8} e^{-3.34 \times 10^{-4}t} \quad (6)$$

and at 100°C it is

$$\text{rate } 100^\circ\text{C} = 1.04 \times 10^{-6} e^{-1.27 \times 10^{-3}t} + 1.95 \times 10^{-7} e^{-4.36 \times 10^{-4}t} \quad (7)$$

The correlation coefficients at all temperatures are better than 99%.

Table I summarizes the rate constants for DAP drying in a low-pressure argon purge using the flowing-afterglow technique. A typical drying curve is shown

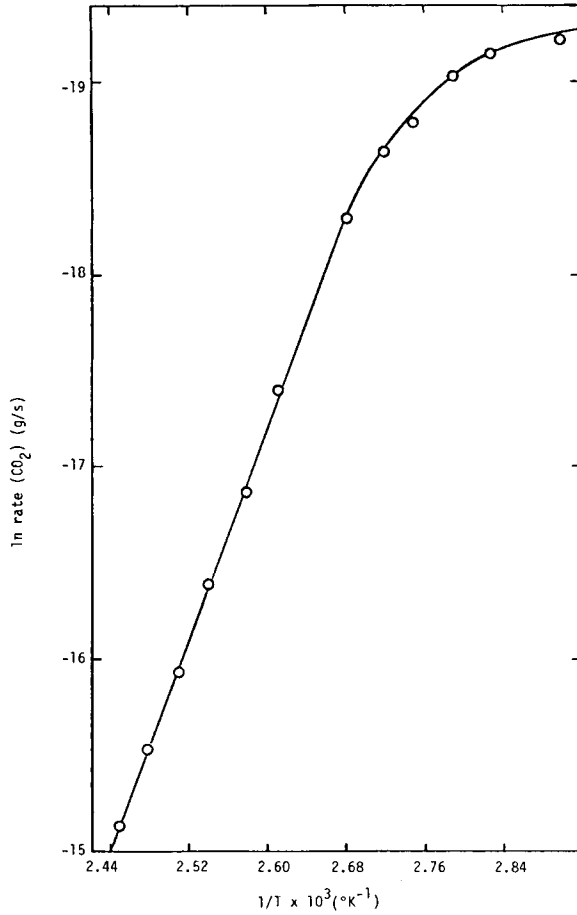


Fig. 7. Carbon dioxide from DAP.

in Figure 6. The most striking result from these data is the complete lack of a significant temperature coefficient (a near zero activation energy) for k_1 . A finite activation energy seems to exist for the k_2 process relative to the k_1 process be-

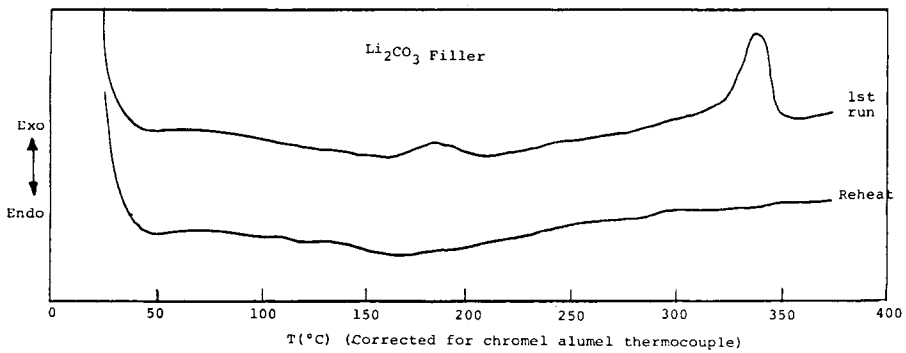


Fig. 8. DTA scans of DAP composite.

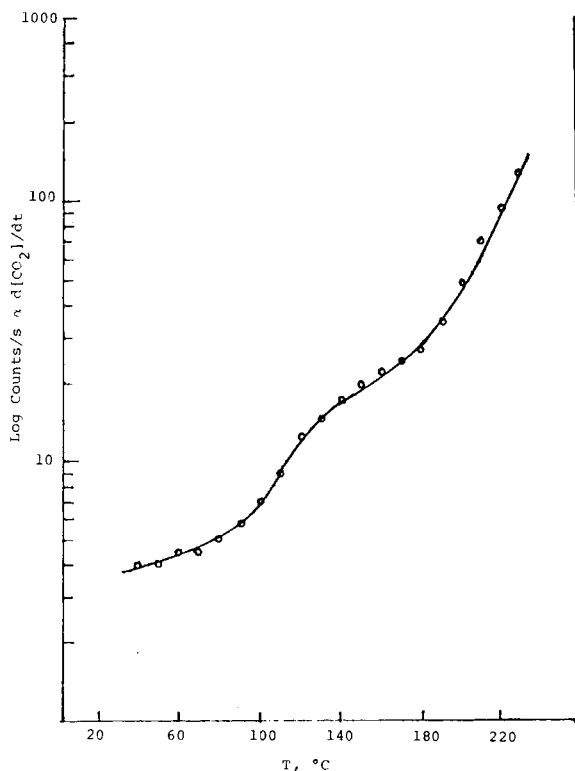


Fig. 9. Afterglow discharge analysis of Estane 5703 thermal degradation.

cause k_1/k_2 decreases with increasing temperature. Repeated drying and equilibration at 10% RH for the same sample showed that both rate constants increased with each heat treatment by as much as a factor of 2.

From the slope of $\log(\text{rate vs. time})$ one can obtain $1/2.3\beta$, where β is the time constant. It is related to the drying rate and thickness of the part by

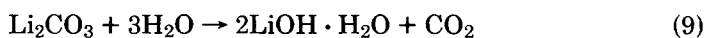
$$\log(\text{rate})_t = -\frac{t}{2.3\beta} + \log(\text{rate})_0 \quad (8)$$

where $\beta = h^2/D^2$, t is time, h is thickness of the part (cm) (critical dimension), and D is the diffusion constant. Using the data from 60°C the diffusion constant was calculated to be $1.19 \times 10^{-1} \text{ cm}\cdot\text{s}^{-1/2}$.

It was found that there were three sources of CO_2 evolution in the DAP composite: (1) continued curing or crosslinking of the polymer at ambient temperatures; (2) reaction of the Li_2CO_3 filler with water; and (3) probable decomposition of the peroxide catalyst used in the curing process. A plot of rate versus reciprocal temperature is shown in Figure 7.

The DTA scans showed an endotherm beginning at approximately 120°C in the first heating that was not present in the second heating. This indicated an undercured condition. The DTA scans are shown in Figure 8. This reaction had an energy of activation of 9.7 kcal/mol as determined using flowing-afterglow data.

The second source of CO_2 was the reaction of water with lithium carbonate



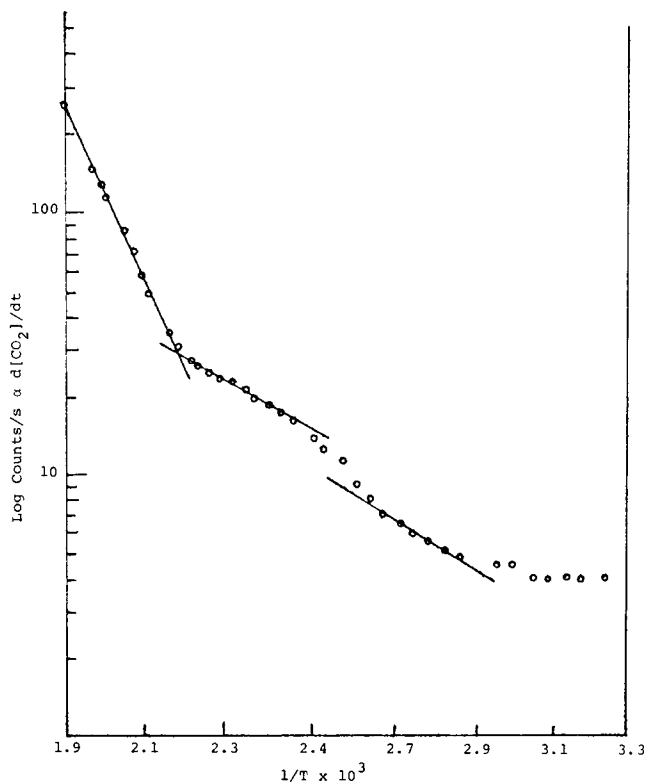


Fig. 10. Arrhenius plot of Estane 5703 thermal degradation.

This reaction was dominant at approximately 100°C and indicated that a phase change was occurring by “spurts” of CO₂. This reaction can be seen at approximately 160°C in the DTA scan in Figure 8.

A third reaction had an energy of activation of 38 kcal/mol, a typical value for a peroxide catalyst decomposition.

Estane 5703

Estane 5703 yielded only CO₂ as a decomposition produce between 35°C and 234°C on a single heating. Figure 9 illustrates the raw data in counts/s [$\alpha d(\text{CO}_2/dt)$] vs. temperature; Figure 10 shows the Arrhenius plot. Above 65°C three distinct processes are discernible. The Arrhenius expressions and appli-

TABLE II
Rate Equations

Material	Product	$k_1 = A_1 e^{-E_i/RT}$	Temp range (°C)
Estane 5703	CO ₂	$k_1 = (3.5 \times 10^4) e^{-4600/RT}$	75–110
		$k_2 = (2.7 \times 10^4) e^{-4140/RT}$	127–183
		$k_3 = (2.2 \times 10^{10}) e^{-15,100/RT}$	183–234

cable temperature ranges are present in Table II. The transitions at 75°C and 183°C (Fig. 10) correlate with two transitions in the DTA scan; the first is an endotherm, which is a softening point, and the second is a very broad exotherm, probably decomposition.

CONCLUSIONS

The flowing-afterglow technique can be used to study the thermal stability of polymeric materials. Using this technique, one can monitor the volatile thermal decomposition products and obtain fast qualitative and quantitative information. The technique measures small amounts of evolved gases. It is a dynamic analysis in which the rate of reaction is proportional to the amount of the evolved gas. An Arrhenius treatment can be used, and changes in mechanism are readily seen. This technique allows one to detect the species that are causing an endotherm or exotherm in more conventional thermal analysis techniques, such as DTA. Comparisons between the kinetic parameters over comparable temperature ranges indicate the regions of mechanism change and allow qualitative comparisons of relative thermal stability. This method affords the opportunity to study low-temperature decomposition processes and to extend the useful range of conventional thermal techniques.

References

1. G. W. Taylor and E. J. Dowdy, "Method and Apparatus for Detecting and Measuring Trace Impurities in Flowing Gases," U.S. Pat. 4,148,612, (1979).
2. C. B. Collins and W. W. Robertson, *Spectrochim. Acta*, **19**, 747 (1967).
3. C. B. Collins and W. W. Robertson, *J. Chem. Phys.*, **40**, 701 (1964).
4. J. F. Prince, C. B. Collins, and W. W. Robertson, *J. Chem. Phys.*, **40**, 2619 (1964).
5. A. L. Schmeltekopf and H. P. Broida, *J. Chem. Phys.*, **39**, 1261 (1963).
6. D. H. Stedman and D. W. Setser, *Prog. React. Kinet.*, **6**, 193 (1971).
7. D. H. Stedman and D. W. Setser, *Chemical Applications of Metastable Rare-Gas Atoms*, Pergamon, Oxford, 1971.
8. G. W. Taylor and G. A. Andrews, *Proceedings of the Fifth Symposium on Chemical Problems Related to Explosive Stability*, Institute of Combustion, Stockholm, Sweden, p. 297 (1979).

Received January 19, 1981

Accepted May 4, 1981